JOURNAL OF GEOPHYSICAL RESEARCH, VOL. 94, NO. B2, PAGES 1655–1664, FEBRUARY 10, 1989

Displacement of Surface Monuments: Vertical Motion

FRANK K. WYATT

Institute of Geophysics and Planetary Physics, University of California, San Diego, La Jolla

Several measurements of vertical ground motion at Piñon Flat Observatory, California, indicate the overall weakness and instability of the Earth's weathered surface with respect to the underlying rock. Cumulative long-period motions of order 0.5 mm per year dominate these records, though smaller elastic deformations caused by precipitation loading, atmospheric loading, and tidal strains are evident at higher frequencies; all of these help to characterize the near-surface material. The long-period records suggest that near-surface weathering is the dominant influence on monument motion, at least at this site on crystalline rock in a semi-arid environment. Rainfall loading gives an average vertical modulus of 2.6 GPa for the material in the uppermost 26 m of the ground, compared with 88 GPa for granite under moderate confining stress; atmospheric loading gives similar results but indicates the ground is permeable to airflow at periods longer than a few hours. Earth tide records show Poisson's ratio to be 0.09 in contrast to the normative range of 0.2–0.25, establishing that horizontal strains couple only weakly into vertical ones, so that vertical strains near the surface are a poor measure of areal strain. The form of the ground-surface displacement power spectrum indicates that analyses of geodetic surveys would be improved with the inclusion of a monument-positioning error budget that increases with time. Because of ground instability, and the generally small rate of crustal tectonic motions, deeply emplaced monuments will be needed for observational programs designed to detect short-term changes in crustal deformation over baselengths of order 10 km and less.

INTRODUCTION

Direct measurements of crustal deformation are limited to observations on, or very near, the ground surface—most often between monuments specifically designed for repeated surveying. Near the ground surface, weathering alters the once competent rock mass to a weakened state, making it an especially noisy place for such measurements. The size of the displacement noise is small enough, and scale of long-term deformations sufficiently broad, that averages of the deformation over large areas and long times generally give useful results [e.g., *Savage*, 1983]. However, over distances of 10 km and less (often comparable to the depth of seismicity), and for time scales of years and shorter, monument instability can be the limiting noise factor. Understanding and quantifying monument stability is thus essential for interpreting results from the more detailed studies of crustal deformation.

This paper on vertical monument motion is intended to complement an earlier one on horizontal motions [*Wyatt*, 1982], and reports on measurements not available then. All of the observations considered here are from Piñon Flat Observatory (PFO), located in southern California between the San Jacinto and San Andreas fault zones. Details of the geological setting are described in the earlier paper. In brief, the site is an upland erosional surface inclined to the southwest with a 3% slope. Its geomorphology suggests that the 12-km^2 flat is a pediment, whose base level is defined by a line of rock exposures along its southwest edge. A layer of sand about 0.3 m thick covers crystalline rock composed of biotite-rich hornblende granodiorite. *Wyatt* [1982] and recent vertical seismic profiles (J. Fletcher, personal communication, 1987) show a linear increase of P wave velocity from 0.5 km/s at the surface to 2 km/s at a depth of 15–20 m, indicative of weakened rock in this range. Below this depth the velocities tend toward values more characteristic of solid granite at low confining pressures (3.5 to 5.5 km/s). The deepest vertical displacement measurements reported on here extend to depths of only 26.5 m, roughly the same depth as the water table.

The most important set of measurements affected by millimeter-size vertical motions is precise geodetic leveling [*Vaníček et al.*, 1980]. For over a century, spirit leveling between widely spaced bench marks has provided most of the evidence for what is known about vertical ground deformations—from regions of active faulting and volcanism to areas of groundwater withdrawal. As to sources of noise, leveling studies by *Savage et al.* [1979] and *Reilinger et al.* [1984] found that the observed ground tilt spectrum has most of its energy at short spatial wavelengths, and suggest elastic warping of the ground as the probable cause. Such signals arise from the coupling of thermal stresses, or regional stresses, into ground tilt, through topography or material inhomogeneities. The results from this study, however, suggest that inelastic processes are more important.

Continuously recording strainmeters and tiltmeters are another class of measurements requiring stable bench marks [*Agnew*, 1986]. These are observatory-based instruments meant to record deformations over distances less than 1 km, with precisions approaching 1 part in 10^{10}. Here the need for exceptionally stable monuments is obvious: motions of only 0.1 mm/yr correspond to strain or tilt rates of 10^{-6} yr^{-1} on 100-m-long instruments. This is much larger than most tectonic signals and, because only a pair of monuments are involved, there is no network averaging to suppress the monument-displacement noise. *Savage* [1983] shows that strain rates in the western United States are of order $1–3 \times 10^{-7}$ yr^{-1}; instrument stability, including attachment to the ground, must be substantially better than this to record crustal deformations faithfully.

The records presented in this paper are from long baselength tiltmeters and from other instruments specifically designed to measure bench mark stability. Long baselength tiltmeters [*Wyatt et al.*, 1984] provide a precise measure of elevation changes between monuments separated by as much as 1 km. (Greater separation is possible, but not generally practical.) To identify those monument motions distinct from tectonic ones, it is assumed that true tectonic signals are gradual, independent of environmental conditions, and common to colocated instruments, so that any

Paper number 88JB03600.
0148-0227/89/88JB-3600$05.00

unreasonably high tilt rates, or correlations between weather and changes in tilt rate, or tilts appearing only on individual instruments running in parallel with others, are taken as evidence of bench mark instability. The best argument for this reasoning is that correcting the long baselength tilt records for their end-monument motions (measured independently, to shallow depth) removes most occurrences of anomalous tilt.

MEASUREMENTS AND TECHNIQUES

Wyatt [1982] found persistent horizontal motions of order 0.1 mm per year for large gabbro monuments installed at a depth of about 2 m. The largest motions were associated with periods of unusually heavy precipitation, which seem to accelerate the weathering of the underlying rock. *Wyatt* [1982] speculated that if indeed weathering were the controlling factor in monument instability then vertical movements might be even larger than horizontal ones, through ongoing dissolution of the underlying rock column.

As an initial test of this, and as the starting point for the development of an instrument capable of recording tectonic deformations, a 50-m-long tiltmeter was built at PFO in 1979. This used an uninterrupted fluid surface (ideally an equipotential surface) as the reference level, forming a Michelson-Gale tiltmeter [*Beavan and Bilham*, 1977]. The end-monuments were two gabbro columns (1.8 m^3) attached to the Earth at depths of 3.7 m (Figure 1). Differencing the fluid height measurements from each end gives the differential elevation change, or tilt, over the 50-m baseline. The results of this experiment (discussed in the next section) verified the inadequacy of such surface monuments for the recording of tectonic signals.

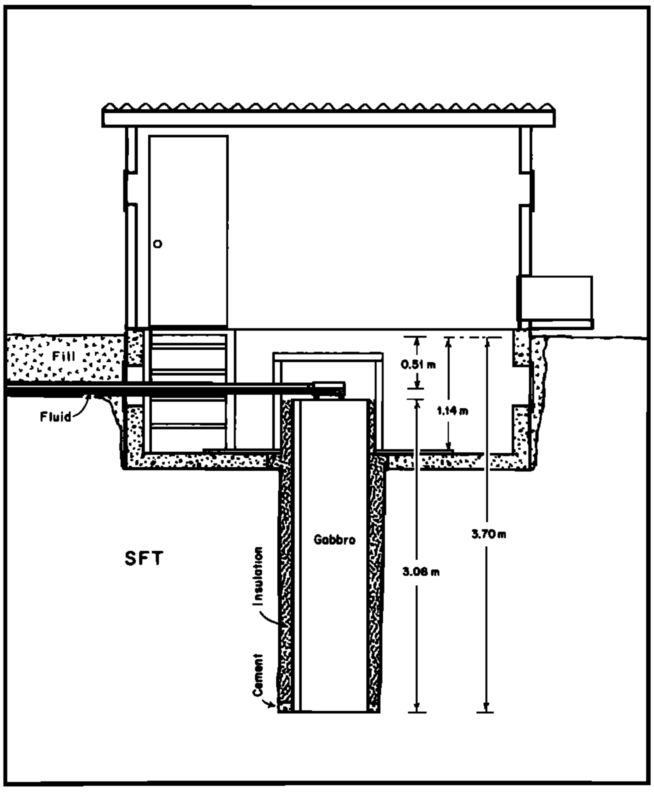

Fig. 1. Side view of one of the end-monuments used in the initial 50-m-long short fluid tiltmeter (SFT). The gabbro columns were cemented into the bottom of large-diameter boreholes and then insulated. The enclosures were temperature controlled.

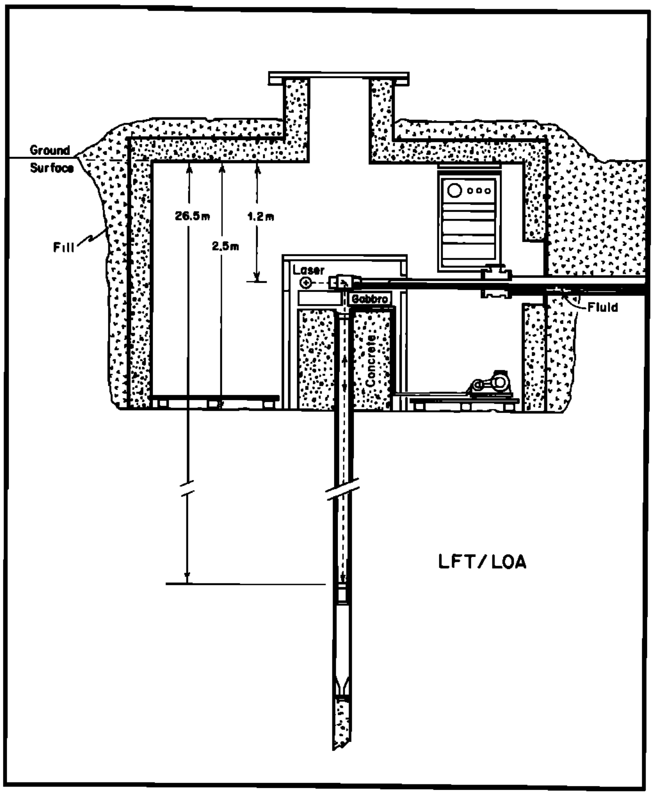

Fig. 2. Side view of one of the end-vaults for the current 535-m-long fluid tiltmeter (LFT), including its 25.3-m vertical laser optical anchor (LOA). Any spurious motions of the gabbro table are registered equally as an apparent height change of the equipotential fluid surface and as a displacement relative to the bottom of the LOA, allowing for their elimination from the tilt record.

The next step was to build a long baselength tiltmeter (535 m) incorporating optical anchors at each end (Figure 2). An optical anchor [*Wyatt et al.*, 1982] is simply an optical interferometer designed to detect any changes in distance between the ground surface and anchoring points at depth. In this application, for the measurement of vertical displacements, the optical anchors extend vertically from the tiltmeter's end-monuments to the bottom of 26.5-m-deep boreholes. Any localized movement of either of the monuments then appears both as a change in tilt (a change in monument height relative to the fluid surface) and as a change in vertical displacement, as recorded by the optical anchor. Subtracting the two optical anchor measurements from the tilt record, itself formed by differencing the fluid level observations from the two ends, corrects for monument instability, at least down to depths of 26.5 m. The monuments for this instrument are gabbro slabs sitting upon 1-m^3 concrete piers which were formed directly on the floors of subsurface vaults. Figure 2 presents the details.

Piñon Flat Observatory is also the site for a large collection of geodetic bench marks. Most of these (about 70) are class B rod marks installed by researchers from the University of California, Santa Barbara (UCSB) in 1979–1980 and surveyed at least annually since then [*Sylvester*, 1984]. Class B marks are small-diameter stainless steel rods driven into the ground a moderate distance [*Floyd*, 1974]. Owing to the toughness of the ground at the observatory, most of the rod marks there extend only to depths of 1 m, much less than the 4-m depth usually achieved for class B

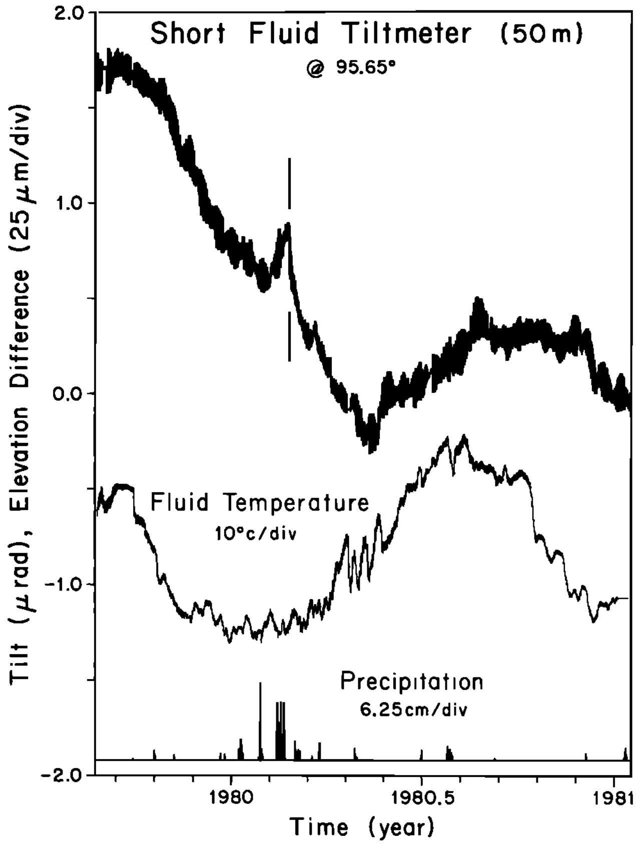

Fig. 3. The complete record from the SFT, including the tiltmeter's fluid temperature. Vertical units are given both in radians of tilt (over 50 m) and as the relative change of height between the two end-monuments. A positive tilt trend indicates ground tipping down at an azimuth of 95.65°, azimuth measured east from north. The broadening of the tilt record is due to the Earth tides.

marks. The UCSB leveling lines also include seven class A bench marks (rods in boreholes, anchored at a depth of 9 m) installed by the National Geodetic Survey (NGS), as well as ties to both the original 50-m tiltmeter and the current 535-m instrument. Five of the class A marks, installed in 1986, are clustered around the west end of the long tiltmeter for direct comparison with its optically anchored monument; a sixth one is at the east end.

OBSERVATIONS

Figure 3 presents the data from the short fluid tiltmeter (SFT) from August 1979 through January 1981, at which time its sensors were removed for use in the long baselength instrument. The records show a cumulative tilt of 1.5μrad, down to the west, much too large to be reflecting broad crustal deformation. The importance of this figure is that it shows an apparent elevation change between the instrument's end-mounts, amounting to 0.08 mm. Even these closely spaced monuments, which must be sharing nearly identical geological and environmental conditions, show substantial differential motion.

The small bump at 1980.15 in Figure 3 (marked by a vertical line) deserves special mention. Its peak corresponds to the time of a moderate earthquake only 13 km away (M_L 5.5 [*Frankel*, 1984]). The bump is not the signature of a regional deformation because colocated strainmeters did not show any unusual signals around this time, at deformation-levels orders of magnitude smaller [*Wyatt*, 1988]. Most likely the onset of this feature is the result of the intense rains which preceded the earthquake, causing water to percolate into the ground around the monuments. Somehow ground shaking seems to have prompted the reversal and eventual dissipation of this rainfall-induced differential displacement, perhaps by promoting drainage in the critical volume just below the monuments.

Vertical displacement records from the West monument (at site Rho) and the East monument (Tau) of the 535-m tiltmeter are presented in Figure 4. Because the final tilt signal from this instrument (when corrected for the end-monument displacements) indicates no more than 0.06 mm/yr of differential monument motion between the endpoints, and this may well be true crustal tilt, it is not displayed here. The most conspicuous event in this figure occurs following the rainstorms of early 1983. These storms led to the rapid uplift of both monuments: at Rho 1 mm, and at Tau 0.4 mm. Actually this event had several phases, not evident on this scale, with the monuments reacting distinctly to successive storms. Because the vault floors are not sealed, once the loose soil immediately surrounding the vault became water saturated, the vaults flooded, but only by a few centimeters. To prevent similar flooding, A-frame roofs were constructed over the vaults late in 1983 (indicated by the asterisks in Figure 4). However, the vault floors remained wet until near the start of 1985 when dehumidifiers were added (cross-hatch symbols). This became necessary because persistently high vault humidity ruined several electronic components. The effect of adding the dehumidifiers was unexpected: both monuments began to settle and have continued to subside since then. An explanation for this is given in the next section.

Further evidence of ground instability comes from small tilt-

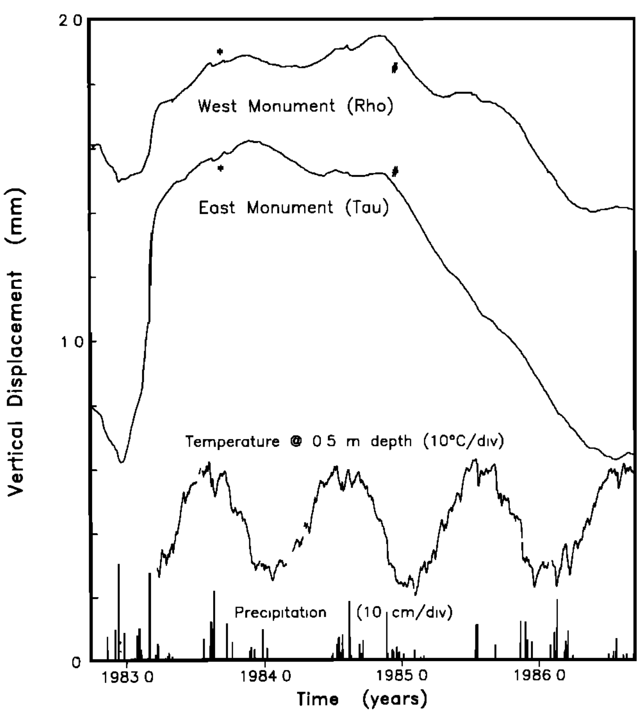

Fig. 4. Four years of vertical displacement records from the optical anchor gauges at the two ends of the LFT. These measurements give the displacement of monuments resting at 2.5-m depth, relative to 26.5 m. Also shown is the ground temperature at a depth of 0.5 m and the daily precipitation. The asterisks show when A-frame weather protection housing was added over the vaults, while the cross-hatch symbols indicate when vault dehumidifiers began operation.

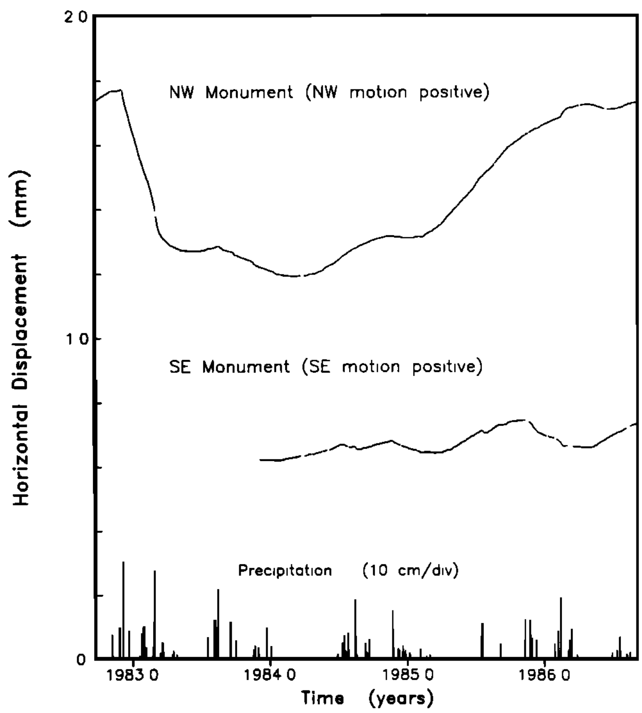

Fig. 5. Horizontal displacement records from horizontal optical anchors for the same period presented in Figure 4. The displacement gauges span roughly the same depth interval as the vertical ones of Figure 4.

meters attached to the end-monuments at Rho and Tau. These sensors show tilts of order 2×10^{-4} rad, with records which look much like the displacement records presented in Figure 4. This tilt corresponds to differential motions of 0.2 mm across the 0.9-m^2 base of the monuments. Such large displacements are surprising considering that the concrete monuments were formed directly on a prepared surface of intact granite which, from the excavation viewpoint at least, was competent. The monuments thus must be averaging the displacements occurring across the surface of this seemingly competent material.

For comparison with the vertical movements of Figure 4, Figure 5 shows the horizontal displacement records for monuments NW and SE of the NW-SE laser strainmeter for the same time period (this plot is a continuation of Figure 8 in *Wyatt* [1982]). Monument NW undergoes a maximum displacement of 0.5 mm relative to 24-m depth, while SE moves about 0.2 mm. Both of these monuments are in vaults of similar construction to those at the ends of long fluid tiltmeter (Figure 2), but without the addition of A-frame roofs or dehumidifiers. The character of the horizontal motions is akin to the vertical ones, but with somewhat less amplitude.

Episodes of rainfall loading are easily identified in the vertical displacement records, providing that the precipitation is large enough and occurs quickly enough that the associated displacements are not lost in the background noise. A close inspection of Figure 4 shows numerous small downward jumps associated with rainfall. These jumps are assumed to reflect the vertical strain induced by an increase in the amount (weight) of water held by the near-surface material. To quantify this response, the rain must not occur so quickly as to cause lateral runoff, nor so slowly that either evaporation allows the water to dissipate between showers or that the surface material becomes saturated, allowing downward flow. At this site the last mechanism does not seem generally important: soil moisture sensors at 1 m show negligible change to all but the most prolonged storms, while the water well records show little clear response to even the biggest rainfalls. Most rainfall is either absorbed by the very near-surface material, whereupon it eventually evaporates, or runs off laterally.

Figure 6 presents an expanded view of the vertical displacements for two representative rainfalls in 1983. This plot includes records from the optical anchors and from two mechanical (invar-rod) displacement gauges developed by researchers from Lamont-Doherty Geological Observatory (LDGO), Columbia University (R. Bilham and J. Beavan, personal communication, 1988; *Wyatt et al.* [1984]); the LDGO W records are from a monument only 11 m distant from Rho, with LDGO E a similar distance from Tau. The response of the adjacent monuments is similar for the two rainstorms, the western monuments showing generally larger displacements (1.1 μm per cm of rainfall) than the eastern ones (0.75 μm per cm). Apparently the ground is stronger in the vicinity of the eastern monuments.

Cross-spectral analysis elucidates two other factors controlling vertical displacements: thermoelastic stresses and barometric loading. Figure 7 shows a heavily averaged power spectrum of the monument motion at Rho along with scaled spectra of the air temperature and atmospheric pressure. Analysis shows that the admittance function is not a constant for either of these factors; rather, the effect they have on vertical displacement is dependent on frequency. For air temperature the influence becomes less at higher frequencies, while for atmospheric loading it is the opposite. At periods of a week the temperature coefficient is 140 nm/°C and at a day only 60 nm/°C; the atmospheric effect is 1.6 nm/Pa at periods of a few days, increasing to 2.8 nm/Pa at 12 hours (S_2), and 3.5 nm/Pa at 6 hours. In Figure 7 the pressure spectrum is plotted using the admittance at S_2, where it is the controlling factor, though pressure also contributes heavily to the S_1 and S_3 spectral peaks. (The pressure amplitudes, for typical atmospheric conditions, are 40 Pa for S_1, 60 Pa for S_2, and 10 Pa for S_3.) The inappropriateness of assuming a constant admittance

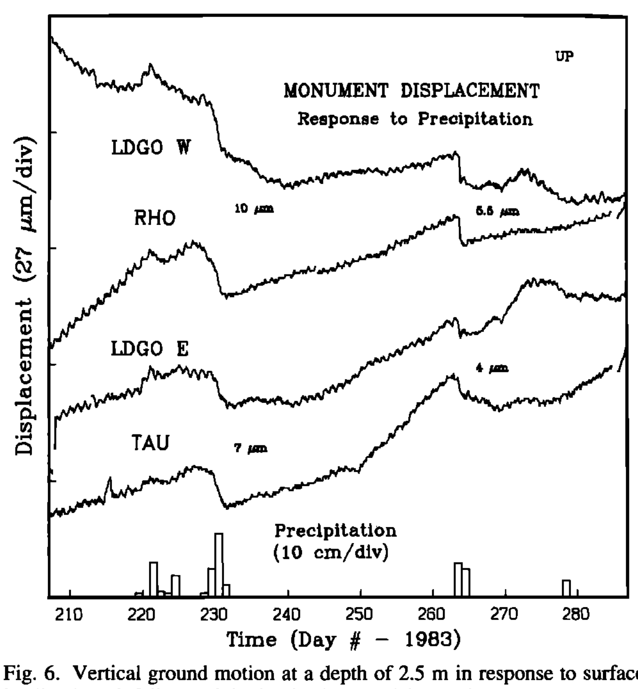

Fig. 6. Vertical ground motion at a depth of 2.5 m in response to surface loading by rainfall. Precipitation is given as daily total.

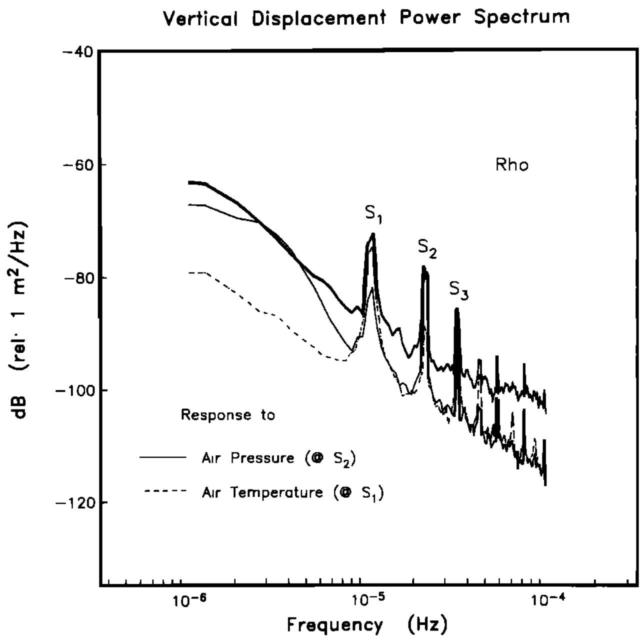

Fig. 7. Vertical displacement power spectral density around 1 cpd, showing contributions from air pressure and air temperature, and assuming constant admittance. In this figure, the air pressure response is taken to be the value determined for a period of 12 hours; the air temperature response is that for 24 hours.

throughout is most evident at frequencies of 3–5 × 10^{-6} Hz, where the scaled, and nominally causative pressure spectrum actually exceeds the observed displacement spectrum slightly. The air temperature is most important at 1 and 3 cycles per day (cpd), but the physical mechanism for this is less certain. The ground temperature is generally taken to attenuate exponentially with depth, depending on the ratio of the depth to a thermal length constant, which itself depends on frequency. At these periods the ground temperature's thermal length constant is about 0.2 m, making simple half-space thermoelastic effects at the vault bottom (2.5 m) vanishingly small, but this ignores those perturbing effects brought about by the vault's presence [e.g., *Agnew*, 1979], and possible topographic/inhomogeneity factors [*Harrison and Herbst*, 1977]. A direct instrumental effect is another candidate mechanism to explain the observed power at 1 cpd and in its harmonics. The instrument temperature coefficient is about 2.5μm/°C (or 15μm/°C if we include the thermal response of the concrete monument), driven by daily variations of about 0.02°C inside the temperature regulated instrument enclosure. Together, air pressure and air temperature cause the daily vertical displacement signals at Rho and Tau (≈1.5μm p-p) to be highly coherent.

The other class of vertical displacement observations at the site are those of the geodetic bench marks. In his 1984 report on bench mark motions at PFO, *Sylvester* [1984] reported apparently random motions for class B rod marks installed at shallow depths (including measurements to a special NGS reference pad, 5 m on a side and 0.3 m thick), with standard deviations about their mean height ranging from 0.5 to 3.2 mm. In seven surveys spanning a period of 3½ years the mean standard deviation was 1.0 ± 0.5 mm. The most stable surveying results (standard deviation of 0.2 mm) came from elevation differences between Rho and Tau (UCSB: 7337 and 7336), between Rho and a class A monument installed by UCSB (UCSB: 05N), and between Rho and the east monument of the original 50-m tiltmeter (UCSB: 7313, or "Grav"); the other end of the original 50-m tiltmeter was not included in the field surveys.

Observation of the newer class A monuments began soon after their installation, in 1986, and they have been resurveyed only a few times since then by each of two groups. Results from this sparse data set show much greater stability, generally with about 0.3-mm standard deviation relative to Rho.

DISCUSSION

This section presents first a description of the mechanisms responsible for long-period vertical ground motions in weathered crystalline rock. These motions are then quantified by means of their power spectrum, allowing for a discussion of the consequences of these observations on programs of crustal deformation measurement. Finally, the records are used to place constraints on various measures of rock and rock-joint moduli.

Weathering and Other Causes of Long-Term Displacement

At this site, the dominant influence on vertical motion of near-surface bench marks is precipitation, through weathering processes activated by changes in soil moisture. The correlation of displacements with periods of heavy precipitation is most clear in the horizontal movement records of *Wyatt* [1982], but it is also quite evident here. The displacement records show long-period excursions only after thorough wetting of the ground, when the top 1 m of the ground becomes saturated, allowing moisture to propagate downward, or during periods of desiccation. Weathering causes the rock to decompose via granular disintegration [*Isherwood and Street*, 1976]; the fully loosened surface material is then eroded downslope, leaving only a thin veneer of soil over the decaying rock. The depth of extensive weathering, or grussification, can be quite deep. *Stierman and Healy* [1985] report evidence of weathering to a depth of 70 m at a setting in California similar to PFO. There they find the change from weakened to competent rock to be quite abrupt and most likely related to water-rock chemistry in the vadose zone—the region above the water table. (Several boreholes at that site gave the water table to be anywhere between 65 and 110 m, thereby showing the difficulty with the very concept of a water table in certain types of fractured crystalline terrain.) They attribute the low strength of the granite to alteration of biotite and chlorite montmorillonite.

Isherwood and Street [1976] ascribe the rapid weathering of biotite-rich rock to the mineral's expansion when subjected to moisture. The expansion of the biotite and the subsequent formation of microfractures in the quartz and feldspars can have the effect of reducing the bulk density of the rock from 2.7 × 10^3 to 2.0 × 10^3 kg/m^3. Figure 4 presents strong evidence for this mechanism: first the end-monuments of the tiltmeter are uplifted by as much as 1 mm following the heavy rainfall, only to show subsidence once the vault and the ground beneath it are dehumidified. Presumably, in the natural course, the ground swells up when wetted, eventually to sink below its initial level (because of partial rock dissolution) as the material returns to its normal moisture content. In this particular instance, the process was apparently frozen in two states: after the rainfalls of early 1983, rain shields prevented subsequent rains from permeating the nearby ground, but (1) the rain shield and the vault itself suppressed the normal evaporative processes, then (2) dehumidifiers were added, causing the underlying material to lose its moisture.

The conditions in the ground immediately under the vault (the first 1–3 m) appear to control the vertical motions; it is this same material that shows the highest degree of weathering. Motions of 1 mm over distances of 1 m imply strains of 10^{-3}. While this is a substantial deformation, it is small compared with the response of the expansive soils discussed in soil mechanics literature [*Chen*, 1975; *Yong and Warkentin*, 1975]. These soils show strains of 10^{-2} in response to 5% changes in soil moisture. By most accounts, the ground at PFO would be considered quite stable.

Soil creep is another candidate for explaining the long-term motions presented in this study, but *Wyatt* [1982] did not find any correlation between lateral ground motions at a few meters depth and ground slope, which rules out this as the controlling mechanism. Since, on the average, the ground is not creeping downslope and yet is weathering, it would seem likely that the long-period vertical motions should exceed the horizontal ones. This is true, but only just so, as shown by comparison of Figures 4 and 5.

All the observations of ground motion at PFO are from depths of 1–3 m, but what might the rate of subsidence be at the ground surface? Averaging over large areas, *Schumm* [1963] found that surface denudation rates are an exponential function of drainage basin relief, the average maximum rate being 1 mm/yr for areas similar to PFO. *Saunders and Young* [1983] discuss downslope soil creep, surface wash, and chemical solution (also called weathering in that paper), along with other mechanisms of ground denudation. The highest rates, again of order 1 mm/yr, are given for semi-arid regions and caused mostly by surface wash, or by intense rainstorms falling on rock poorly protected by vegetation. Indeed they suggest that the rate of 1 mm/yr may represent the threshold which prevents establishment of substantial vegetation cover. Both the thinness of the vegetation and the displacement measurements of the underlying rock at PFO are in accord with this high rate.

As an example of ground motion under other circumstances, *Riley* [1970] reported on long-baseline tiltmeter recordings of land surface deformation from hydrocompaction of moisture-deficient fan deposits. Hydrocompaction occurs when highly porous sediments, above the water table, are rewetted for the first time since deposition, resulting in weakened intergranular bonds and settling under the overburden load—a geological setting much different from PFO. Recognizing the need for vertical anchoring, 46-m-deep invar-type compaction gauges were built at the ends of fluid-level tiltmeters [*Riley*, 1970, 1986]. He found initial ground swelling with increased soil moisture (0.3 mm when the end vaults flooded), a frequency-dependent barometric response (indicating a vertical modulus of 0.25 GPa at periods of a few hours), and thermoelastic effects, all in common to what is found at PFO. Even the hydrocompaction effect, 0.4–0.8 mm of displacement over the 46-m length of the vertical extensometers, was commensurate. In sharp contrast, records from the 30.5-m-long tiltmeters showed differential subsidence of 2.5 mm, even after correction for end-monument motion, indicating substantial displacement below the bottom of the extensometers.

Power Spectral Levels and their Consequences for Measurements of Crustal Deformation

Figure 8 presents the vertical displacement observations of Figure 4 in another form, as their power spectral density. This figure is comparable to Figure 9 of *Wyatt* [1982] and shows that the vertical displacement power levels are about 6 dB higher (a factor of 2 in amplitude) than the power levels forming the horizontal spectrum, except at the lowest frequencies where both data sets show considerable scatter. Generally, the spectra display the same

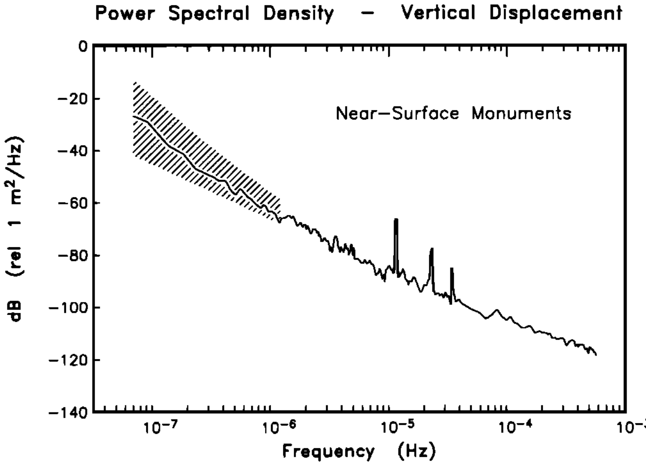

Fig. 8. Several decades of the vertical displacement power spectrum for near-surface monuments, showing the general dependence on frequency (f^{-2}) characteristic of Brownian motion. The shaded region indicates the typical range of results for the lower frequencies; at higher frequencies the spectra show little scatter.

power law, power inversely proportional to the frequency squared, which is descriptive of one-dimensional Brownian motion, or a random-walk process. *Wyatt* [1988] gives the standard deviation for such processes as a function of the interval T between observations. Over the frequency band where the displacement power spectrum may be written as $P(f) = P_0(2\pi f)^{-2}$, the standard deviation of displacement is given by $\sigma = (\frac{1}{2}P_0T)^{1/2}$. Here this is valid above 10^{-6} Hz (about 12 days), with $P_0 = 1.8 \times 10^{-17}$ m^2/s giving $\sigma = 3.0 \times 10^{-9}\,(\mathrm{m\,s^{-1/2}})\,T^{1/2}$, or $\sigma = 3.3\,\mu$m in 2 week's time. The equivalent standard deviation for horizontal motion at 2 weeks is just one half of this, or $1.7\,\mu$m. This formulation progressively underestimates the standard deviation at times longer than this, as the spectrum diverges from the simple f^{-2} power law, indicating even greater energy at the longer periods. Empirical studies show that for $P(f) = P_0(2\pi f)^{-\alpha}$, σ may be approximated by $(\frac{1}{2}P_0T^{\alpha-1})^{1/2}$, for α in the range 1.5–2.6. Over intervals of 5 months, which coincides with the lowest frequency results given in Figure 8, displacements may thus amount to something between 0.01 and 0.24 mm, corresponding to the lower and upper bounds of that plot. Many more data are needed to define the spectral levels at periods of a year and more.

Strictly Brownian motion ($\alpha = 2$) is governed by the diffusion equation [*Lavenda*, 1985], providing another useful way to understand monument motion. The root-mean-square of a particle's displacement is given by $(2DT)^{1/2}$, where D is the diffusion coefficient ($D = \frac{1}{4}P_0$). A monument may therefore be considered as an individual particle, albeit a macroscopic one, diffusing through the ground. The diffusion coefficient for this, 10^{-17} m^2/s, is roughly a factor of 10^{10} smaller than the coefficient for most other individual "particles" in nature (e.g., thermal diffusivity, as mentioned in the next section).

Despite the general recognition of the effects of bench mark instability on inferred vertical crustal motions [e.g., *Karcz et al.*, 1976], most reviews of geodetic leveling make little mention of it. This is true because, in some sense, adequate long-term coupling to the earth is outside the domain of leveling (most statistical evaluations are based on discrepancies between forward and backward runs, or loop misclosure), and because bench mark stability is generally adequate for surveying purposes. Also, for baselengths longer than 10 km, monument motions are usually small compared with long-period tectonic signals.

For measurements of crustal deformation over shorter distances, whether by leveling or from tiltmeters, monument stability is crucial. *Savage et al.* [1979] give the variance in tilt for leveling between two bench marks a distance L apart as

$$\sigma_{\text{tilt}}^2 = 2\alpha^2/L + 2\beta^2/L^2 \qquad (1)$$

where $(2\alpha^2 L)^{1/2}$ is the standard deviation in the relative change of elevation due to measurement error, and $(2\beta^2)^{1/2}$ is due to bench mark instability from all sources (e.g., simple decoupling, thermoelastic/inhomogeneity effects). The first term comes from the statistically independent random errors which accumulate according to the square root of the survey distance, $\alpha = 1.6 \times 10^{-5}$ m$^{1/2}$ (or 0.5 mm/km$^{1/2}$) for the highest order modern leveling [*Vaniček et al.*, 1980]. The second term clearly depends on the type of monuments used and the environmental and geological setting. Based on the assumption of uniform tilting, *Savage et al.* [1979] find β = 0.25 mm for class B rod marks driven to a depth of 5–6 m at sites in central California; *Sylvester* [1984] gives a somewhat larger value of 1.0 mm for the generally shallower marks at PFO. Using β = 0.5 mm and taking L to be 1 km (such that the two terms of (1) contribute roughly equally) gives σ = 1.0 μrad, a large uncertainty in the measurement of tectonic deformation.

In searching for an explanation for the high degree of nonuniform movement exhibited by adjacent bench marks, *Savage et al.* [1979] review several earlier studies of small-aperture leveling arrays. They note that large-aperture arrays tend to average out this short-wavelength noise, presumably because the tilt episodes seen on the smaller arrays are not coherent across the entirety of the larger ones. The preferred mechanism for this is elastic vertical displacements of order 1 mm caused by the coupling of thermoelastic, tectonic, or other strains into vertical motions through topographic or local material inhomogeneities [e.g., *Harrison and Herbst*, 1977].

Weathering of the ground surface is an alternative explanation, consistent with the results from PFO. In this context, weathering may be considered simply as causing poor coupling of the monuments to the Earth's crust, though at the ground surface itself this might not be evident. The presumption of weathering as the cause of long-period, short-wavelength tilt noise has a most important implication. The form of the displacement power spectrum indicates that for any finite interval T, the process will be dominated by energy with frequency near $1/T$ and that all parts of the series will be correlated (not statistically independent); as Figure 4 makes clear, averages over longer and longer time periods do not necessarily converge to fixed values [*Mandelbrot and McCamy*, 1970]. The form of (1) is thus incomplete and should be modified to include a time dependence of the standard deviation due to cumulative monument instability:

$$\sigma_{\text{tilt}}^2 = 2\alpha^2/L + 2\beta_0^2/L^2 + 2\beta_t^2/L^2 \qquad (2)$$

where β_0 is meant to include only those monument-positioning errors not increasing with time (e.g., reoccupation errors, true decoupling, cyclic elastic displacements), and $\beta_t = (\frac{1}{2} P_0 T^{\alpha-1})^{1/2}$. In fact, at PFO, elastic effects seem to be insignificant.

Sylvester [1984] presents the time history of vertical motions for representative monuments at PFO. Excluding the first of the two 1982 surveys, most all the plots in this article show a correlation of sequential observations, as would be expected for samples of Brownian motion. Since the variation in these displacements far exceeds the theoretical random survey error (the first term in (1)), we may use these records to estimate P_0. For the better UCSB class B monuments at PFO β_t is about 0.65 mm in a year's time, giving $P_0 = 2.7 \times 10^{-14}$ m^2/s (assuming $\alpha = 2$), and for the most stable monuments, emplaced at several meters depth, β_t is about 0.18 mm in a year, or $P_0 = 2.1 \times 10^{-15}$ m^2/s.

Estimates of Rock Properties

Seismic velocities in the upper 20 m at PFO are well below those for solid rock. This could be due to the results of weathering, to inherent rock porosity (microcracks, scale 1–100 μm [*Birch*, 1961]), or because of numerous weak joints. In their study of jointing and seismic velocities in fractured granite, *Moos and Zoback* [1983] found that while large-scale joints are important in explaining the increase of velocity with depth (perhaps by promoting chemical and mechanical alteration near their surfaces), composition and microscopic properties of the rock itself are the main factors governing velocity. This suggests that weathering or naturally occurring microcracks are the primary mechanisms affecting the near-surface material.

The nonlinear stress-strain behavior of intact rock at low confining stress is generally ascribed to microcracks [*Walsh*, 1965*a*; *Walsh and Grosenbaugh*, 1979]. As confining stresses are increased, the cracks close and the rock eventually becomes nearly linearly elastic. But for crystalline rock at pressures less than 100 MPa (i.e., above depths of 3.8 km in the Earth, assuming lithostatic load only) the effect of microcrack opening is dramatic: Young's modulus changes from nearly 70 GPa under pressure to 20 GPa [*Brace*, 1965], and Poisson's ratio falls from 0.2–0.25 to near zero [*Walsh*, 1965*b*; *Jaeger and Cook*, 1976]. Complicating matters is whether dynamic tests (monitoring seismic velocities of mega-Hertz pulses) or static tests are used to measure these parameters; the effects of open cracks cause dynamic techniques to be in error by as much as several hundred percent at atmospheric pressure [*Simmons and Brace*, 1965]. Thus the relationship between seismic velocities and the true elastic moduli of near-surface rocks is poorly determined, except that since seismic waves are less likely to cause actual displacements at crack faces than do static loads, dynamic tests give results biased toward greater stiffness; they tend to provide an upper limit on the rock's moduli. Poisson's ratio ν, rigidity μ, and Young's modulus E may be written in terms of compression and shear velocities V_P and V_S, and density ρ:

$$\nu = \frac{1}{2}\frac{(V_P/V_S)^2 - 2}{(V_P/V_S)^2 - 1} \qquad \mu = \rho V_S^2 \qquad E = 2\mu(1+\nu)$$

For the values of seismic velocities at PFO (J. Fletcher, personal communication, 1987) this gives $E \sim 1$ GPa and $\nu = 0.10$ in the depth range 0–7.5 m, with $E \sim 7$ GPa and $\nu = 0.11$ between 7.5 and 15 m, jumping to $E \sim 50$ GPa, $\nu = 0.22$, between 15 and 35 m. The change in magnitude of Young's modulus provides good evidence that the rock below about 20 m is sound (not friable), while the rapid increase in Poisson's ratio argues for confining stresses higher than lithostatic. (For confining stresses near atmospheric, ν is expected to be low, and seismic velocities actually tend to underestimate it [*Jaeger and Cook*, 1976].) It is also possible that the jump in ν and E are, in part, a consequence of moisture saturation conditions likely prevailing below 15 m.

Rainfall loading gives a better determination of the average rock rigidity. *Farrell* [1972] reviews the equations for deformations of an elastic half-space caused by surface loads. For an arbitrary distribution of surface pressure P acting on a homogeneous elastic half-space, the vertical strain at the surface is given by $\varepsilon_z = -P / 2(\lambda + \mu)$, where λ is Lamé's constant ($\lambda = 2\mu\nu / (1 - 2\nu)$). As discussed earlier, rainfall is assumed to be absorbed in the upper 2.5 m of the ground, above the floor of the vaults. Using an average of the loading displacements given previously, dividing by the length of the optical anchor below the vault floor (24 m), and converting the rainfall into a load, gives a vertical modulus ($-P/\varepsilon_z$) of 2.6 GPa. Assuming for the moment $\nu = 0.1$ (so $\lambda = 0.25\mu$), we have $E = 2.3$ GPa for Young's modulus over the depth range 2.5–26.5 m, a value in reasonable accord with the seismically determined values.

Atmospheric loading should cause the same signals as does precipitation, but cross-spectral analysis between the air pressure and vertical displacements shows a diminishing effect toward low frequencies. Again taking $\nu = 0.1$, and dividing by the instrument length, we may convert the observed displacement values to estimates of Young's modulus. Here, the ground apparently becomes much stiffer at low frequencies, being 6.4 GPa for 6-hour periods and 13.9 GPa at a few days. These values, but especially the long-period one, seem to contradict the rainfall loading results, but may be explained as the consequence of airflow into the permeable ground. An infinitely permeable rock mass would display infinite strength with respect to air pressure loading, because no net downward pressure would be created on its surface. The permeability of the ground surface means long-period air pressure signals will not deform it as much as short-period pressure fluctuations.

The annual temperature swing is another cause of cyclical vertical motions. *Harrison and Herbst* [1977] show that the (upward) vertical displacement at depth z, due to an imposed temperature variation $T = T_0 \cos \omega t$ on the surface of a homogeneous half-space, is

$$U(z) = \tfrac{1}{2} \frac{1+\nu}{1-\nu} \beta \, T_0 \, k^{-1} e^{-kz} \, \{\cos(\omega t - kz) + \sin(\omega t - kz)\}$$

where t is time, ω frequency (in rad/s), β the coefficient of linear expansion, and $k = (\omega/2\kappa)^{1/2}$, κ the thermal diffusivity. The thermal wave number k for $\kappa = 7.5 \times 10^{-7}$ m^2/s (typical for surface rocks) is $[2.7 \text{ m}]^{-1}$ at periods of a year. Based on buried ground temperature sensors at PFO, the effective amplitude of the annual surface temperature cycle is estimated to be 9° C. (Because the uppermost layer of the ground at PFO is a particularly good insulator the true surface temperature cycle is somewhat bigger than this.) With $\beta = 8 \times 10^{-6}$ °C^{-1} and $\nu = 0.1$, this gives the annual cycle at a depth of 3 m (just below the vault floor) as 0.11 mm (p-p), delayed about 110 days from the temperature cycle. A close inspection of Figure 4 shows that this model fits the observations fairly well. For monuments installed at depths of only 1 m (e.g., the class B rod marks at PFO) the theoretical signal would be 0.23 mm, roughly twice as large.

The assumption of Poisson's ratio has little impact on the foregoing results, nevertheless we can derive an independent estimate for it too. At the traction-free surface of homogeneous elastic half-space the areal strain ($\varepsilon_A = \varepsilon_1 + \varepsilon_2$, where ε_1 and ε_2 are any two orthogonal measures of strain on the free surface) is related to the vertical strain by

$$\varepsilon_z = \frac{-\nu}{1-\nu} \varepsilon_A$$

For $\nu = 0.25$, its nominal value, $\varepsilon_z = -0.33\,\varepsilon_A$. Figure 9 shows the power spectra of both the vertical strain at Tau (where the ground is somewhat stiffer than at Rho) and the areal strain from a data series analyzed similarly. The areal strain is from the unanchored NS and EW 732-m-long laser strainmeters at the site (discussed by *Agnew* [1986]) and so gives the areal strain at 3-m depth, averaged over an area roughly 1 km^2 which encompasses Tau. Taking Poisson's ratio to be 0.25, and in the absence of any other vertical strain-generating mechanism, we should expect the vertical strain to be everywhere 0.33 of the areal strain spectrum, or, in decibels, 9.6 dB less than the areal strain. Figure 9 shows the vertical strain is instead generally greater, indicating that the vertical strain continuum must be noise of nontectonic origin. This also follows from the long-term vertical displacement records of Figure 4, which, when converted to strain, give rates fully 2 orders of magnitude larger than other measures of Earth strain at the site. In Figure 9 the power spectral levels are nearly equal at lines S_1 and S_3, but this is an artifact of the vertical displacement's sensitivity to air temperature (discussed earlier). The spectral levels also overlap at S_2, but here the apparent agreement is caused by response to air pressure. Only at M_2 (12.42-hour period) is the vertical strain exceeded by the areal strain by more than 10 dB and showing a clear response above the vertical-strain noise continuum. For Rho and Tau this difference in M_2 spectra levels is 21.5 and 18.5 dB, respectively. Taking the mean value of 20 dB, or $\varepsilon_z = -0.1\,\varepsilon_A$, implies $\nu = 0.09$.

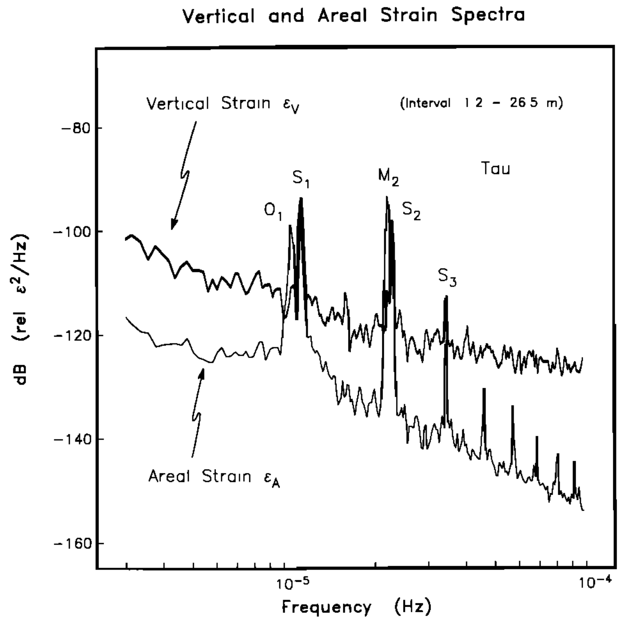

Fig. 9. Comparison of vertical and areal strain spectra for the records from PFO. For Poisson's ratio of 0.25 the areal strain spectrum should uniformly exceed the vertical strain by 9.6 dB, which it does not, indicating the generally high noise level of near-surface vertical strain.

Theoretical arguments based on the opening of microcracks at low pressures [*Walsh*, 1965b; *Kemeny and Cook*, 1986] predict that a linear relationship should exist between Poisson's ratio and Young's modulus, which is given by $\nu = (\nu_0/E_0)E$, where the subscripted terms are the limiting values obtained at very high confining stresses. *Jaeger and Cook* [1976] plot observations of this which show considerable scatter. The results here, of quite low values for ν and E near the surface, are generally consistent with this relationship.

Movements on fractures and joints are another mechanism affecting vertical displacements. Although even the meaning of joints in the uppermost layers is ambiguous, below some depth they are likely the controlling factor. *Engelder* [1987] defines joints as being "a break or crack in rock displaying opening displacements and no appreciable shear displacement." *Twidale* [1982] notes that most all granites near the Earth's surface are fractured, often in joint systems that parallel the ground surface, the result of erosional unloading. In their studies of borehole seismic velocities, *Stierman and Kovach* [1979] and *Moos and Zoback* [1983] found a systematic discrepancy between in situ seismic velocities (spanning intervals of 1–2 m) and laboratory estimates of pressurized core samples from wells with numerous fractures, indicating the influence of fractures on intact properties. In another study of six wells drilled in granite to depths of 25 m and in three wells drilled to about 1 km, *Seeburger and Zoback* [1982] found only a slight decrease in the number of fractures per unit length with increasing depth. At PFO, various borehole logs show fracture spacing S averaging from 1.5 to 5 m, similar to the results reported by *Seeburger and Zoback* [1982]. Fractures are thus important and pervasive.

Bandis et al.'s [1983] laboratory study provides an excellent empirical description of rock-joint deformation. Jointing's contribution to the overall moduli of a rock mass may be computed by knowledge of the rock-joint's stiffness (both normal and in shear), together with only a few other observations of joint closure and joint spacing [e.g., *Fossum*, 1985]. The normal stiffness k_n, at a given normal stress σ_n, is defined as $d\sigma_n/da$, where a is the joint aperture. *Walsh and Grosenbaugh* [1979] show that the normal joint stiffness should be proportional to normal stress, $k_n = \xi \sigma_n$, and report $\xi = 1.2 \times 10^4\ \mathrm{m}^{-1}$ for jointed granite. We may therefore use an estimate of normal joint stiffness at some depth and knowledge of average joint spacing to determine the effective modulus for any interval in the vertical column.

In a study of PFO ground deformation, caused by transient lowering of the water table, *Evans and Wyatt* [1984] found $k_n = 20$ GPa/m for a joint at 100-m depth, under 36 m of lithospheric load (26 kPa/m, above the water table) and 64 m of reduced load (16 kPa/m, loading reduced by hydrostatic pressure in the affected joint). This gives a total effective load of 1.92 MPa, and this implies $k_n(z) = 1.0 \times 10^4 \sigma_n(z)$, in good agreement with the value of ξ above.

To determine the effective vertical modulus of a column L (assuming the joints to be nearly horizontal and with even spacing S), we need only sum the contributions of the individual joints. Equation (3), based on the definitions for the vertical modulus and normal joint stiffness, gives the general expression for this between depths of z_1 and z_2:

$$\frac{-P}{\varepsilon_z} = (z_2 - z_1)\left[\sum_{l=z_1/S+1}^{z_2/S} \frac{1}{k_n(lS)}\right]^{-1} \qquad z_2 - z_1 > S \tag{3}$$

This is most easily applied for jointing above the water table where it is assumed that $\sigma_n(z) = \rho g z$. From the surface to some depth z the vertical modulus is then

$$-P/\varepsilon_z = \xi S \rho g z \left[\sum_{l=1}^{z/S} \frac{1}{l}\right]^{-1}$$

with the upper few cracks dominating the result. (Note that the infinite harmonic series $\Sigma_{l=1}^{\infty} 1/l$ is divergent.) For $\xi = 10^4\ \mathrm{m}^{-1}$, $S = 2$ m, and $z = 26$ m, this equation gives $-P/\varepsilon_z = 4.2$ GPa and $E = 3.7$ GPa (when $\nu = 0.1$). This result is essentially the same as the value of E determined by rainfall loading, lending some credence to the form of the stiffness versus normal stress law used in the model, irrespective of whether very near-surface deformations actually occur at joints or are dispersed within zones of alteration near them. For rocks below 30 m at PFO, where the rock is strong except for jointing, the general form of (3) ought to apply.

CONCLUSIONS

Weathering of the ground seems to be the primary factor controlling the long-period displacement of surface monuments, at least at this one site on crystalline rock in a semi-arid environment. The general consistency of survey leveling results [e.g., *Savage et al.*, 1979; *Sylvester*, 1984; and *Reilinger et al.*, 1984] and near-surface deformational measurements [*Wyatt et al.*, 1988] from a range of locations would suggest this observation is broadly applicable. Once the surface material is sufficiently wetted to allow the moisture to migrate downward, accelerated weathering of the rock begins, often lasting for months, with large displacements persisting throughout the desiccation period.

For measurements of tectonic deformation, the apparently chaotic motions of very near-surface monuments may be generally so large as to become the limiting factor in detecting short-term signals occurring over distances of 10 km and less. Averaging over many monuments, while certain to improve matters, ultimately will be limited by any systematic component in the ground's response to environmental changes. The form of the vertical displacement power spectrum suggests that, in the analysis of field observations, including an error term dependent on time (its square root or a slightly higher power) should improve estimates of true ground deformation. Most all the records discussed here indicate anchoring to depth as the solution to the problem of monument instability. The superior performance of class A geodetic marks at PFO testifies to this. Their design, rod marks isolated from the surface and extending to 10-m depths [*Floyd*, 1974], demonstrates the geodetic community's long-standing recognition of the need for deep anchoring. As the weathering of surface rocks may extend beyond even this depth, still deeper anchoring may be needed for observational programs seeking very high accuracy over short periods and short spatial distances.

Finally, vertical strain measurements near the ground surface are not likely to yield useful estimates of tectonic strain. The records from the near surface are quite noisy, being at least an order of magnitude noisier than the equivalent horizontal strain, while below the water table another mechanism comes into play: horizontal jointing permits changes in the water pressure to induce large vertical strains [*Evans and Wyatt*, 1984]. Also, the inherently low value of Poisson's ratio at low confining stress means that horizontal strains couple only weakly into vertical strains.

Acknowledgments. This research was supported by grants from the National Science Foundation and the U.S. Geological Survey. I wish to thank Arthur Sylvester for the many years of precise leveling data, Roger Bilham and John Beavan for the use of observations from their long base tiltmeter at the site, and William Kaula, Ross Stein, and the National Geodetic Survey for the installation and monitoring of the class A bench mark cluster. Leo Weuve saw to the integrity of all the field records, for which I am indebted. Keith Evans, in addition to his most thorough review of the initial manuscript, introduced me to the subject of joint stiffness in rock, and so deserves credit for several of the ideas presented here. Duncan Carr Agnew, John Langbein, and Ross Stein each provided particularly valuable comments on earlier versions of this article.

REFERENCES

Agnew, D. C., Strain tides at Piñon Flat: Analysis and interpretation, Ph.D. thesis, Univ. of Calif., San Diego, 1979.

Agnew, D. C., Strainmeters and tiltmeters, *Rev. Geophys.*, *24*, 579–624, 1986.

Bandis, S. C., A. C. Lumsden, and N. R. Barton, Fundamentals of rock joint deformation, *Int. J. Rock Mech. Min. Sci. Geomech. Abstr., 20*, 249–268, 1983.

Beavan, R. J., and R. Bilham, Thermally induced errors in fluid tube tiltmeters, *J. Geophys. Res., 82*, 5699–5704, 1977.

Birch, F., The velocity of compressional waves in rocks to 10 kilobars, 2, *J. Geophys. Res., 66*, 2199–2224, 1961.

Brace, W. F., Some new measurements of linear compressibility of rocks, *J. Geophys. Res., 70*, 391–398, 1965.

Chen, F. H., *Foundations on Expansive Soils*, pp. 280, Elsevier, New York, 1975.

Engelder, T., Joints and shear fractures in rock, in *Fracture Mechanics of Rock*, edited by B. K. Atkinson, pp. 27–69, Harcourt Brace Jovanovich, San Diego, Calif., 1987.

Evans, K., and F. Wyatt, Water table effects on the measurement of earth strain, *Tectonophysics, 108*, 323–337, 1984.

Farrell, W. E., Deformations of the earth by surface loads, *Rev. Geophys., 10*, 761–797, 1972.

Floyd, R. P., Geodetic bench marks, *NOAA Manual NOS NGT 1*, 50 pp., Natl. Oceanic and Atmos. Admin., Washington, D. C., 1974.

Fossum, A. F., Elastic properties for a randomly jointed rock mass, *Int. J. Rock Mech. Min. Sci. Geomech. Abstr., 22*, 467–470, 1985.

Frankel, A., Source parameters of two $M_L = 5$ earthquakes near Anza, California, and a comparison with an Imperial Valley aftershock, *Bull. Seismol. Soc. Am., 74*, 1509–1527, 1984.

Harrison, J. C., and K. Herbst, Thermoelastic strains and tilts revisited, *Geophys. Res. Lett., 4*, 535–537, 1977.

Isherwood, D., and A. Street, Biotite-induced grussification of the Boulder Creek Granodiorite, Boulder County, Colorado, *Geol. Soc. Am. Bull., 87*, 366–370, 1976.

Jaeger, J. C., and N. G. W. Cook, *Fundamentals of Rock Mechanics*, 2nd ed., 585 pp., Chapman and Hall, London, 1976.

Karcz, I., J. Morreale, and F. Porebski, Assessment of benchmark credibility in the study of recent vertical crustal movements, *Tectonophysics, 33*, T1–T6, 1976.

Kemeny, J., and N. G. W. Cook, Effective moduli, non-linear deformation and strength of a cracked elastic solid, *Int J Rock Mech. Min. Sci. Geomech Abstr., 23*, 107–118, 1986.

Lavenda, B. H., Brownian motion, *Sci. Am., 252*, 70–85, 1985.

Mandelbrot, B. B., and K. McCamy, On the secular pole motion and the Chandler wobble, *Geophys. J. R. Astron. Soc., 21*, 217–232, 1970.

Moos, D., and M. D. Zoback, In situ studies of velocity in fractured crystalline rocks, *J. Geophys. Res., 88*, 2345–2358, 1983.

Reilinger, R., M. Bevis, and G. Jurkowski, Tilt from releveling: An overview of the U.S. data base, *Tectonophysics, 107*, 315–330, 1984.

Riley, F. S., Land-surface tilting near Wheeler Ridge, southern San Joaquin Valley, California, *U.S. Geol. Surv. Prof. Pap., 497-G*, 1970.

Riley, F. S., Developments in borehole extensometry, Land Subsidence, Proceedings of the Third International Symposium on Land Subsidence, Venice, Italy, *IASH, Pub., 151*, 169–186, 1986.

Saunders, I., and A. Young, Rates of surface processes on slopes, slope retreat and denudation, *Earth Surface Proc. Landforms, 8*, 473–501, 1983.

Savage, J. C., Strain accumulation in western United States, *Annu. Rev. Earth Planet. Sci., 11*, 11–43, 1983.

Savage, J. C., W. H. Prescott, J. F. Chamberlain, M. Lisowski, and C. E. Mortensen, Geodetic tilt measurements along the San Andreas Fault in central California, *Bull. Seismol. Soc. Am., 69*, 1965–1981, 1979.

Schumm, S. A., The disparity between present rates of denudation and orogeny, *U.S. Geol. Surv. Prof. Pap., 454-H*, 1963.

Seeburger, D. A., and M. D. Zoback, The distribution of natural fractures and joints at depth in crystalline rock, *J. Geophys. Res., 87*, 5517–5534, 1982.

Simmons, G., and W. F. Brace, Comparison of static and dynamic measurements of compressibility of rocks, *J. Geophys. Res., 70*, 5649–5656, 1965.

Stierman, D. J., and J. H. Healy, A study of the depth of weathering and its relationship to the mechanical properties of near-surface rocks in the Mojave Desert, *Pure Appl. Geophys., 122*, 425–439, 1985.

Stierman, D. J., and R. L. Kovach, An in situ velocity study: The Stone Canyon well, *J. Geophys. Res., 84*, 672–678, 1979.

Sylvester, A. G., Leveling precision and bench mark motions, Piñon Flat Observatory, California, *J. Geophys. Res., 89*, 7949–7956, 1984.

Twidale, C. R., *Granite Landforms*, Elsevier, New York, 1982.

Vaníček, P., R. O. Castle, and E. I. Balazs, Geodetic leveling and its applications, *Rev. Geophys., 18*, 505–524, 1980.

Walsh, J. B., The effect of cracks on the compressibility of rocks, *J. Geophys. Res., 70*, 381–389, 1965*a*.

Walsh, J. B., The effect of cracks in rocks on Poisson's ratio, *J. Geophys. Res., 70*, 5249–5257, 1965*b*.

Walsh, J. B., and M. A. Grosenbaugh, A new model for analyzing the effects of fractures on compressibility, *J. Geophys. Res., 84*, 3532–3536, 1979.

Wyatt, F., Displacements of surface monuments: Horizontal motion, *J. Geophys. Res., 87*, 979–989, 1982.

Wyatt, F. K., Measurements of coseismic deformation in southern California 1972–1982, *J. Geophys. Res., 93*, 7923–7942, 1988.

Wyatt, F., K. Beckstrom, and J. Berger, The optical anchor—A geophysical strainmeter, *Bull. Seismol. Soc. Am., 72*, 1707–1715, 1982.

Wyatt, F., R. Bilham, J. Beavan, A. Sylvester, T. Owen, A. Harvey, C. Macdonald, D. Jackson, and D. Agnew, Comparing tiltmeters for crustal deformation measurement—A preliminary report, *Geophys. Res. Lett., 11*, 963–966, 1984.

Wyatt, F. K., S.-T. Morrissey, and D. C. Agnew, Shallow borehole tilt: A reprise, *J. Geophys. Res., 93*, 9197–9201, 1988.

Yong, R. N., and B. P. Warkentin, *Soil Properties and Behavior*, pp. 449, Elsevier, New York, 1975.

F. K. Wyatt, Institute of Geophysics and Planetary Physics, University of California, San Diego, La Jolla, CA, 92093

(Received April 4, 1988;
revised August 18, 1988;
accepted August 31, 1988.)